Electronic Supplementary Material (ESI) for Molecular BioSystems.

Dimerization-based Control of Cooperativity

Mehdi Bouhaddou and Marc R. Birtwistle[#]

Icahn School of Medicine at Mount Sinai, Department of Pharmacology and Systems Therapeutics, New York, NY 10029, USA

[#]Corresponding author: marc.birtwistle@mssm.edu

Supplementary Information

Table of Contents

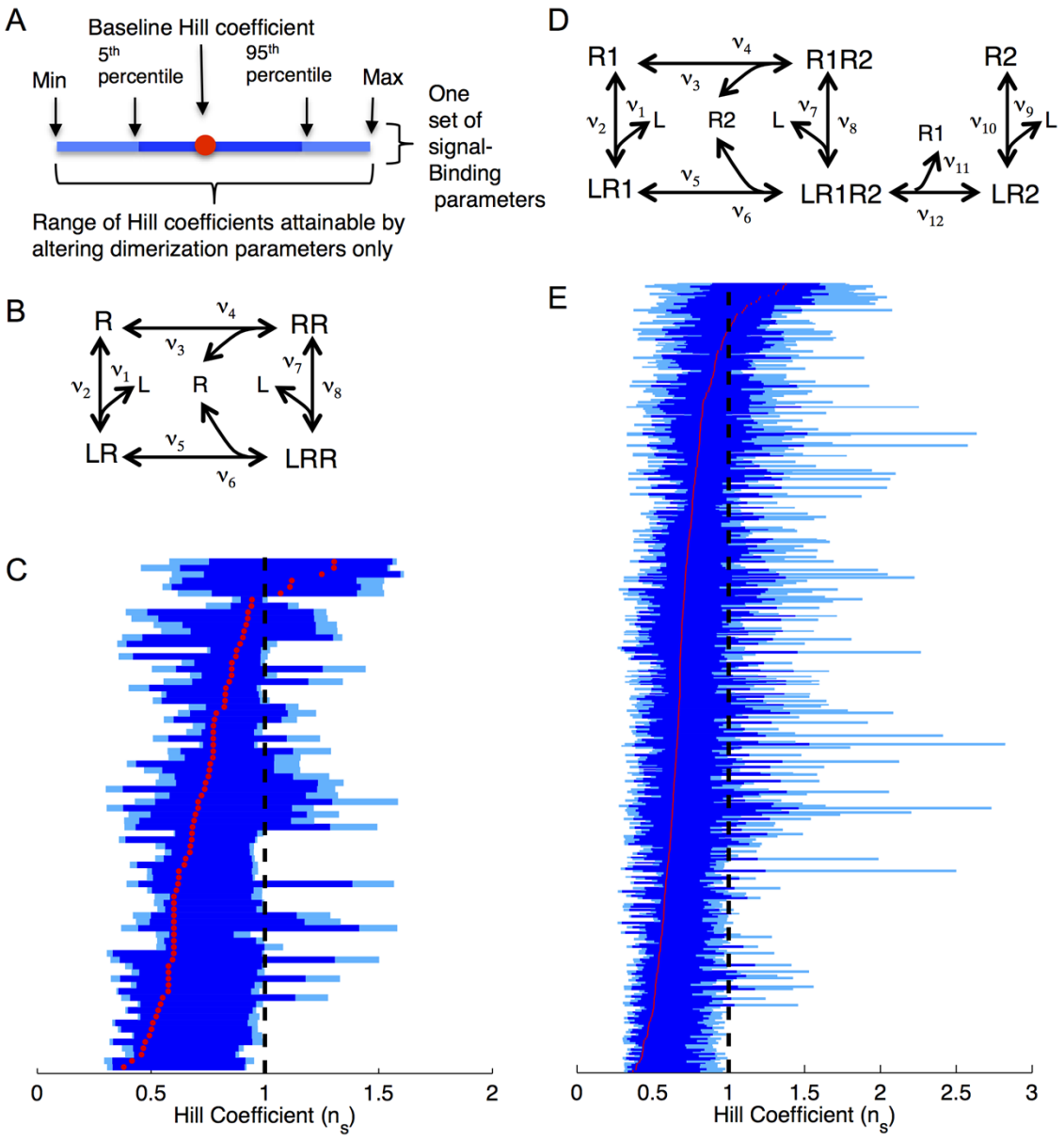

Figure S1. The effect of dimerization on cooperativity behavior for a bivalent-ligand interacting with a homodimer or heterodimer receptor.
(A) Graphical description of each horizontal bar (in C and E). Each horizontal bar corresponds to 3^4 (in C) or 3^6 (in E) simulations and spans the range of Hill coefficients attainable by altering dimerization rate constants (to 0.1, 1, or 10 s^{-1} or $nM^{-1}s^{-1}$) while keeping signal binding rate constants fixed. The dark blue section of each bar denotes Hill coefficients between the 5th and 95th percentiles and the light blue tips span the remaining 5% on either side. Each bar contains a single red dot, indicating the "baseline" Hill coefficient when all dimerization rate constants are set to unity. (B) Kinetic scheme for bivalent-ligand interacting with a homodimer receptor. (C) Results for model shown in B, displaying Scatchard n_s Hill coefficients. (D) Kinetic scheme for bivalent-ligand interacting with a heterodimer receptor. (E) Results for model shown in D, displaying Scatchard n_s Hill coefficients.

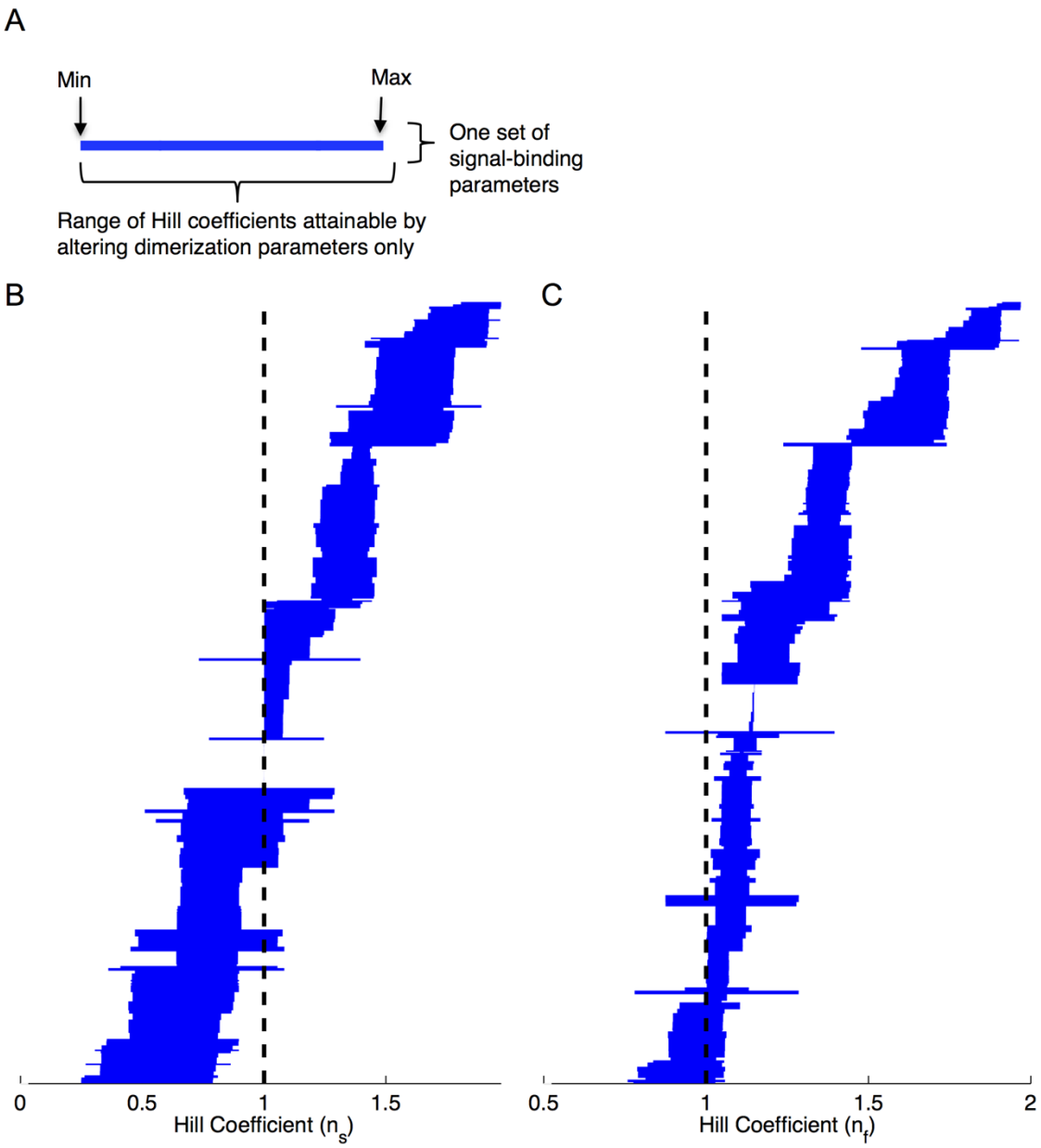

Figure S2. Effect of dimerization affinity on cooperativity behavior using simulations that satisfy detailed balance.
(A) Graphical description of each horizontal bar (in B and C). Each horizontal bar comprises 3^6 (729) simulations that satisfy detailed balance (see Methods for more info) and spans the range of Hill coefficients attainable by altering dimerization rate constants while keeping signal-binding rate constants fixed. The bar extends from the minimum to the maximum Hill coefficient for each set. (B) Results for Scatchard Hill coefficients (n_s). (C) Results for functional Hill coefficients (n_f). Sets are sorted according to the midpoint between the minimum and maximum Hill coefficients.

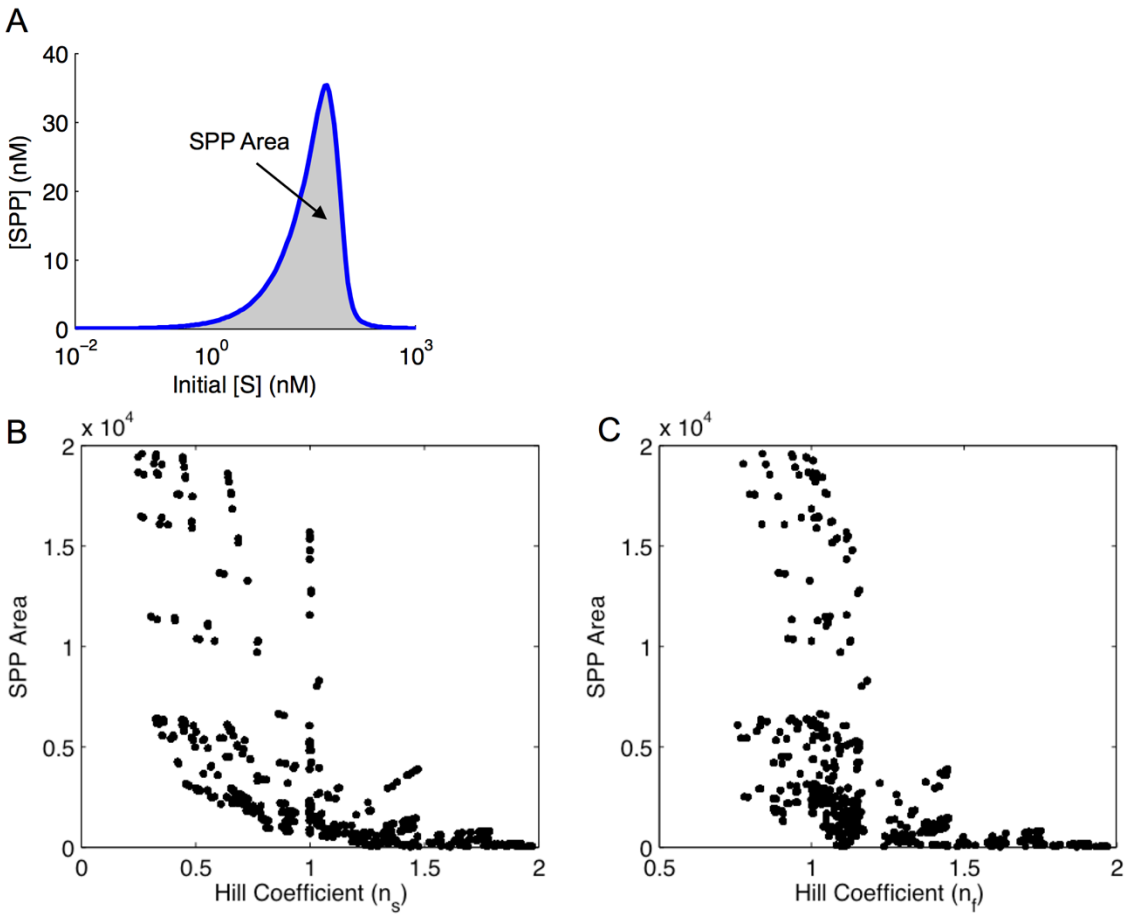

Figure S3. Relationship between stoichiometrically asymmetric dimer accumulation and cooperativity using simulations that satisfy detailed balance.
(A) An example of how "SPP area" (shaded region) is calculated. (B) Scatterplot showing the correlation between Scatchard Hill coefficients (n_s) and their corresponding SPP areas for each of the 3^{12} (531,441) simulations that satisfy detailed balance (see Methods for more info). The correlation is highly significant (ρ=-0.62, $p<0.001$). (C) Scatterplot showing the correlation between functional Hill coefficients (n_f) and their corresponding SPP areas for each of the 3^{12} simulations that satisfy detailed balance. The correlation is highly significant (ρ=-0.47, $p<0.001$).

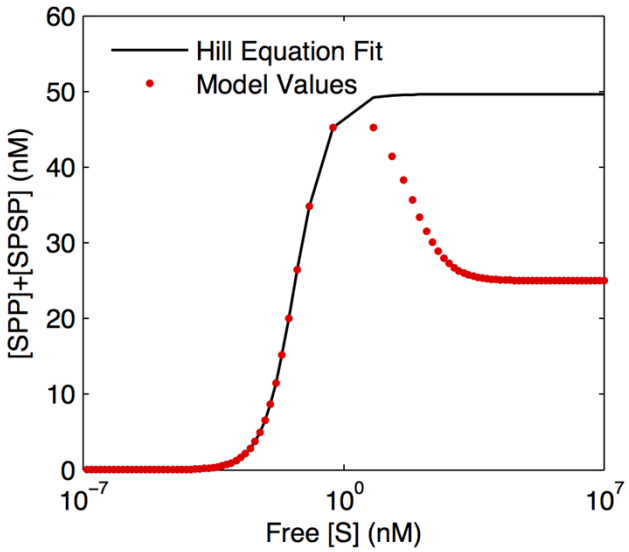

Figure S4. For functional analyses, the Hill equation is fit to the first portion of the dose-response curve.
Model-simulated values are depicted in red dots. The Hill equation fit to the model output is shown with a solid black line. The fit, and the resulting functional Hill coefficient, is calculated using only values prior to the maximum of the model-simulated dose-response curve.

Supplementary Table S1. The ordinary differential equations for the model depicted in Figure 1A.

$$\frac{d[S]}{dt} = k_1[SP] + k_7[SPP] + 2 \cdot k_9[SPSP] - k_2[S][P] - 2 \cdot k_8[S][PP] - k_{10}[SPP][S]$$

$$\frac{d[P]}{dt} = k_1[SP] + 2 \cdot k_3[PP] + k_5[SPP] - k_2[S][P] - 2 \cdot k_4[P]^2 - k_6[SP][P]$$

$$\frac{d[SP]}{dt} = k_2[S][P] + k_5[SPP] + 2 \cdot k_{11}[SPSP] - k_1[SP] - k_6[SP][P] - 2 \cdot k_{12}[SP]^2$$

$$\frac{d[SPSP]}{dt} = k_{10}[SPP][S] + k_{12}[SP]^2 - 2 \cdot k_9[SPSP] - k_{11}[SPSP]$$

$$\frac{d[PP]}{dt} = k_4[P]^2 + k_7[SPP] - k_3[PP] - 2 \cdot k_8[S][PP]$$

$$\frac{d[SPP]}{dt} = k_6[SP][P] + 2 \cdot k_8[S][PP] + 2 \cdot k_9[SPSP] - k_5[SPP] - k_7[SPP] - k_{10}[SPP][S]$$

Supplementary Table S2. The ordinary differential equations for the model depicted in Figure 1B.

$$\frac{d[S]}{dt} = k_1[SP] - k_2[S][P]$$

$$\frac{d[P]}{dt} = k_1[SP] + k_5[SPP] - k_2[S][P] - k_6[SP][P]$$

$$\frac{d[SP]}{dt} = k_2[S][P] + k_5[SPP] - k_1[SP] - k_6[SP][P]$$

$$\frac{d[SPP]}{dt} = k_6[SP][P] - k_5[SPP]$$

Supplementary Table S3. The ordinary differential equations for the model depicted in Figure 1C.

$$\frac{d[S]}{dt} = k_1[SP] - k_2[S][P]$$

$$\frac{d[P]}{dt} = k_1[SP] - k_2[S][P]$$

$$\frac{d[SP]}{dt} = k_2[S][P] + 2 \cdot k_{11}[SPSP] - k_1[SP] - 2 \cdot k_{12}[SP]^2$$

$$\frac{d[SPSP]}{dt} = k_{12}[SP]^2 - k_{11}[SPSP]$$

Supplementary Table S4. The ordinary differential equations for the bivalent-ligand interacting with homodimer receptors model depicted in Figure S1B-C.

$$\frac{d[L]}{dt} = k_1[LR] + k_7[LRR] - k_2[L][R] - k_8[L][RR]$$

$$\frac{d[R]}{dt} = k_1[LR] + 2 \cdot k_3[RR] + k_5[LRR] - k_2[L][R] - 2 \cdot k_4[R]^2 - k_6[LR][R]$$

$$\frac{d[LR]}{dt} = k_2[L][R] + k_5[LRR] - k_1[LR] - k_6[LR][R]$$

$$\frac{d[RR]}{dt} = k_4[R]^2 + k_7[LRR] - k_3[RR] - k_8[L][RR]$$

$$\frac{d[LRR]}{dt} = k_6[LR][R] + k_8[L][RR] - k_5[LRR] - k_7[LRR]$$

Supplementary Table S5. The ordinary differential equations for the bivalent-ligand interacting with heterodimer receptors model depicted in Figure S1D-E.

$$\frac{d[L]}{dt} = k_1[LR_1] + k_7[LR_1R_2] + k_9[LR_2] - k_2[L][R_1] - k_8[L][R_1R_2] - k_{10}[L][R_2]$$

$$\frac{d[R_1]}{dt} = k_1[LR_1] + k_3[R_1R_2] + k_{11}[LR_1R_2] - k_2[L][R_1] - k_4[R_1][R_2] - k_{12}[LR_2][R_1]$$

$$\frac{d[R_2]}{dt} = k_3[R_1R_2] + k_5[LR_1R_2] + k_9[LR_2] - k_4[R_1][R_2] - k_6[LR_1][R_2] - k_{10}[L][R_2]$$

$$\frac{d[LR_1]}{dt} = k_2[L][R_1] + k_5[LR_1R_2] - k_1[LR_1] - k_6[LR_1][R_2]$$

$$\frac{d[LR_2]}{dt} = k_{10}[L][R_2] + k_{11}[LR_1R_2] - k_9[LR_2] - k_{12}[LR_2][R_1]$$

$$\frac{d[LR_1R_2]}{dt} = k_6[LR_1][R_2] + k_8[L][R_1R_2] + k_{12}[LR_2][R_1] - k_5[LR_1R_2] - k_7[LR_1R_2] - k_{11}[LR_1R_2]$$

$$\frac{d[R_1R_2]}{dt} = k_4[R_1][R_2] + k_7[LR_1R_2] - k_3[R_1R_2] - k_8[L][R_1R_2]$$